

Biofouling control by phosphorus limitation strongly depends on the assimilable organic carbon concentration

Javier, Luisa; Farhat, Nadia M.; Desmond, Peter; Linares, Rodrigo Valladares; Bucs, Szilárd; Kruithof, Joop C.; Vrouwenvelder, Johannes S.

DOI

[10.1016/j.watres.2020.116051](https://doi.org/10.1016/j.watres.2020.116051)

Publication date

2020

Document Version

Final published version

Published in

Water Research

Citation (APA)

Javier, L., Farhat, N. M., Desmond, P., Linares, R. V., Bucs, S., Kruithof, J. C., & Vrouwenvelder, J. S. (2020). Biofouling control by phosphorus limitation strongly depends on the assimilable organic carbon concentration. *Water Research*, 183, Article 116051. <https://doi.org/10.1016/j.watres.2020.116051>

Important note

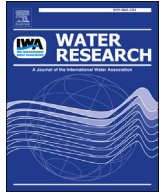
To cite this publication, please use the final published version (if applicable).
Please check the document version above.

Copyright

Other than for strictly personal use, it is not permitted to download, forward or distribute the text or part of it, without the consent of the author(s) and/or copyright holder(s), unless the work is under an open content license such as Creative Commons.

Takedown policy

Please contact us and provide details if you believe this document breaches copyrights.
We will remove access to the work immediately and investigate your claim.



Biofouling control by phosphorus limitation strongly depends on the assimilable organic carbon concentration

Luisa Javier ^{a,1}, Nadia M. Farhat ^{a,*}, Peter Desmond ^{b,c}, Rodrigo Valladares Linares ^d, Szilárd Bucsa ^a, Joop C. Kruithof ^e, Johannes S. Vrouwenvelder ^{a,f}

^a King Abdullah University of Science and Technology (KAUST), Water Desalination and Reuse Center (WDRC), Division of Biological and Environmental Science and Engineering (BESE), Thuwal, 23955-6900, Saudi Arabia

^b Eawag, Swiss Federal Institute of Aquatic Science and Technology, 8600, Dübendorf, Switzerland

^c ETH Zürich, Institute of Environmental Engineering, 8093, Zürich, Switzerland

^d Renewable Energy Unit, Yucatan Center for Scientific Research (CICY), 43 Street #130, Chuburna de Hidalgo, 97205, Mérida, Yucatan, Mexico

^e Wetsus, European Centre of Excellence for Sustainable Water Technology, Oostergoweg 9, 8911 MA, Leeuwarden, the Netherlands

^f Delft University of Technology, Faculty of Applied Sciences, Department of Biotechnology, Van der Maasweg 9, 2629 HZ, Delft, the Netherlands

ARTICLE INFO

Article history:

Received 17 March 2020
Received in revised form
11 June 2020
Accepted 12 June 2020
Available online 16 June 2020

Keywords:

Biofouling
Seawater desalination
Biofilm structure
Phosphate limitation
Carbon limitation

ABSTRACT

Nutrient limitation is a biofouling control strategy in reverse osmosis (RO) membrane systems. In seawater, the assimilable organic carbon content available for bacterial growth ranges from about 50 to 400 $\mu\text{g C}\cdot\text{L}^{-1}$, while the phosphorus concentration ranges from 3 to 11 $\mu\text{g P}\cdot\text{L}^{-1}$. Several studies monitored biofouling development, limiting either carbon or phosphorus. The effect of carbon to phosphorus ratio and the restriction of both nutrients on membrane system performance have not yet been investigated.

This study examines the impact of reduced phosphorus concentration (from 25 $\mu\text{g P}\cdot\text{L}^{-1}$ and 3 $\mu\text{g P}\cdot\text{L}^{-1}$, to a low concentration of $\leq 0.3 \mu\text{g P}\cdot\text{L}^{-1}$), combined with two different carbon concentrations (250 $\mu\text{g C}\cdot\text{L}^{-1}$ and 30 $\mu\text{g C}\cdot\text{L}^{-1}$), on biofilm development in an RO system. Feed channel pressure drop was measured to determine the effect of the developed biofilm on system performance. The morphology of the accumulated biomass for both carbon concentrations was characterized by optical coherence tomography (OCT) and the biomass amount and composition was quantified by measuring total organic carbon (TOC), adenosine triphosphate (ATP), total cell counts (TCC), and extracellular polymeric substances (EPS) concentration for the developed biofilms under phosphorus restricted (P-restricted) and dosed (P-dosed) conditions.

For both carbon concentrations, P-restricted conditions ($\leq 0.3 \mu\text{g P}\cdot\text{L}^{-1}$) limited bacterial growth (lower values of ATP, TCC). A faster pressure drop increase was observed for P-restricted conditions compared to P-dosed conditions when 250 $\mu\text{g C}\cdot\text{L}^{-1}$ was dosed. This faster pressure drop increase can be explained by a higher area covered by biofilm in the flow channel and a higher amount of produced EPS. Conversely, a slower pressure drop increase was observed for P-restricted conditions compared to P-dosed conditions when 30 $\mu\text{g C}\cdot\text{L}^{-1}$ was dosed. Results of this study demonstrate that P-limitation delayed biofilm formation effectively when combined with low assimilable organic carbon concentration and thereby, lengthening the overall membrane system performance.

© 2020 Elsevier Ltd. All rights reserved.

1. Introduction

Advanced water treatment technologies, such as pressure-

driven membrane systems, emerged over the past 50 years to satisfy the increasing global freshwater demand (Elimelech and Phillip, 2011). Membrane filtration installations grew in number and capacity, with a primary focus on different strategies to reduce the energy demand and environmental impact (Greenlee et al., 2009). Biofilm occurrence in membrane systems is considered inevitable, and the excessive growth of biofilms (biofouling) in membrane systems is a significant problem. Biofouling results in

* Corresponding author.

E-mail address: nadia.farhat@kaust.edu.sa (N.M. Farhat).

¹ Shared first authorship.

unacceptable losses in membrane performance: increasing the feed channel pressure drop (PD), reducing membrane flux and/or solute rejection, increasing energy requirements and water production cost (Vrouwenvelder et al., 2007).

Extensive research has been carried out to prevent and control biofouling (Flemming, 2020; Matin et al., 2011). The most commonly applied biofouling control strategy is feedwater pre-treatment to reduce organic nutrient content and to remove bacterial cells. However, even after removal of 99.9% of the microorganisms in the feed water, active microbial cells remain, which grow and multiply consuming biodegradable substances present in the feed water of the membrane installation (Flemming, 1997). Other biofouling control strategies are (i) membrane surface modification, which may delay biofilm formation, but does not prevent biofouling, (ii) feed spacer design, which reduces the effect of accumulated biomass and enhances the cleanability of the membrane module, and (iii) chemical/mechanical membrane cleaning, which is effective in temporarily restoring membrane performance (Bucs et al., 2018; Sanawar et al., 2018).

Nutrient limitation is considered a biofouling control strategy in reverse osmosis membrane systems, with assimilable carbon limitation as the first considered mitigation strategy (Allan et al., 2002; Chandy and Angles, 2001). In seawater, the assimilable organic carbon content available for bacterial growth ranges from 50 to 400 $\mu\text{g C}\cdot\text{L}^{-1}$ (Abushaban et al., 2019). Limitation of nitrogen and phosphorus in the feed water has also been considered to restrict microbial growth in membrane modules (Desmond et al., 2018; Jacobson et al., 2009; Kim et al., 2014; Vrouwenvelder et al., 2010). The phosphorus concentration in seawater ranges from 3 to 11 $\mu\text{g P}\cdot\text{L}^{-1}$, and after water pre-treatment with processes such as coagulation, it may be restricted to values below 1 $\mu\text{g P}\cdot\text{L}^{-1}$ (Jacobson et al., 2009). Several studies reported a mass ratio for carbon (C), nitrogen (N) and phosphorus (P) of at least ~100:23:4.3 for bacterial growth to occur (Burton et al., 2010); indicating that even a minor change in phosphorus concentration in the feed water can have a significant influence on the growth of microorganisms (Miettinen and Vartiainen, 1997).

Phosphorus occurs naturally as different types of phosphate (PO_4^{3-}) (i) ortho-phosphates, (ii) condensed, and (iii) organic phosphates. The soluble form, ortho-phosphate, can be readily used by microorganisms (Vrouwenvelder et al., 2010). The condensed form (meta, pyro, and pylo-phosphate), sometimes referred to as inorganic phosphate, is composed of multiple ortho-phosphate molecules together (Cade-Menun et al., 2018). Lastly, organic phosphates are a class of phosphates which are bound to organic compounds (Dabkowski and White, 2015). Although the condensed and organic phosphates are less available for microbial utilization, they can be converted to ortho-phosphate, increasing the concentration of biologically available phosphorus in water (Lehtola et al., 2001).

It is not well understood how varying the nutrient composition in the feed water affects the biofilm structure and, subsequently, the membrane performance indicators in reverse osmosis (RO) and nanofiltration (NF) modules. Biofilm structure has been studied since the early 1990s using microscopic techniques at a microscale. Some of the principal drawbacks of applying the commonly used microscopic techniques to study membrane biofouling are that these techniques are mainly destructive, with a low axial resolution, and with limitations in laser penetration (Neu et al., 2010). However, in recent years, more focus has been directed towards understanding and analyzing biofilm structures at mesoscale. Optical coherence tomography (OCT) is a non-disruptive imaging technique that recently gained attention in biofilm research (Blauert et al., 2015). OCT is capable of imaging *in-situ* spatially resolved structures on a millimeter-scale with a micrometer

resolution; therefore, OCT is used to compare the structural properties of biofilms (such as density, porosity, thickness, roughness, spatial distribution) grown at different nutritional conditions. Studies have shown that varying the nutrient concentration in the feed water influences the structural properties of biofilms, affecting membrane performance parameters (Derlon et al., 2012; Desmond et al., 2018).

Several studies have been carried out to characterize biofouling development while limiting either carbon or phosphorus concentration in the feed water (Allan et al., 2002; Desmond et al., 2018). However, the effect of restricting both carbon and phosphorus on biofilm development and its impact on the membrane system has not yet been investigated. The objective of this study was to examine the impact of reducing the phosphorus concentration to a low concentration ($\leq 0.3 \mu\text{g P}\cdot\text{L}^{-1}$) on biofilm development in RO systems at two dosed assimilable organic carbon concentrations (250 and 30 $\mu\text{g C}\cdot\text{L}^{-1}$). Morphology and composition of the developed biofilms were examined under phosphorus-restricted (P-restricted, $\leq 0.3 \mu\text{g P}\cdot\text{L}^{-1}$) and dosed (P-dosed, 3 and 25 $\mu\text{g P}\cdot\text{L}^{-1}$) conditions. The effect of varying the nutrient load on membrane system performance (feed channel pressure drop) was monitored to achieve a comprehensive understanding of the biofouling problem and, therefore, its control.

2. Materials and methods

2.1. Experimental setup

A lab-scale experimental setup representative to the practical operation of spiral wound membrane systems was used for this study (Bucs et al., 2016). A cross-flow channel comprising of a membrane sheet and feed flow channel called Membrane Fouling Simulator (MFS) was used for this experiment (Vrouwenvelder et al., 2007).

The setup consisted of a feed water pump, a feed flow meter and controller, a biodegradable nutrient dosage system (pump and controller), a membrane fouling simulator, a back-pressure valve (Bronkhorst, Ruurlo, Netherlands) and a differential pressure sensor (Delta bar, PMD75, Endress + Hauser, Switzerland) to monitor the pressure drop over the flow channel. The system was fed by potable tap water produced by the King Abdullah University of Science and Technology seawater desalination plant (Thuwal, Jeddah, Saudi Arabia). Because the tap water is chlorinated, the feed water was filtered by an activated carbon filter (filter housing model: UPS BB3 [AWF-UPS-3H-20B] cartridges model: sediment-carbon [AC-SC-10-NL]) to remove the residual chlorine, and by two cartridge filters (pore size 4 μm) to remove any particles entering the feed water from the carbon filter. For this study, reverse osmosis produced tap water was selected to ensure an extremely low phosphorus content. Earlier work (Farhat et al., 2018) has shown that dosage of biodegradable nutrients to various water types provided the same bacterial growth yield in seawater as the bacterial growth yield in tap water. Therefore, the results presented in this paper are representative for seawater biofouling as well.

The original MFS has been modified to include an optical glass sight window to allow *in-situ* OCT imaging. The MFS uses a membrane with the dimensions of 20 cm \times 3.5 cm, a 34 mil (864 μm) thick feed channel spacer, taken from a new commercially available spiral wound membrane element (TW30-4040, DOW FILMTEC, USA). The MFS has an inlet and outlet sides allowing cross-flow operation and two orifices for different pressure measurements. The system and water characteristics are representative of biofilm studies, as previously reported by Farhat et al. (2019).

2.2. Operating conditions

The system was operated at a constant pressure of two bar in cross-flow mode. The feed water was pumped through the MFS at a flow rate of 17 L h^{-1} equivalents to a linear flow velocity of 0.18 m s^{-1} , which is representative for practical membrane filtration installations (Bucs et al., 2016). The tap water feeding the MFS had a phosphorus concentration of $\leq 0.3 \mu\text{g P}\cdot\text{L}^{-1}$.

Table 1 shows the experimental conditions. A nutrient stock solution containing sodium acetate, sodium nitrate, and sodium phosphate in a mass ratio of C:N:P of 100:20:10 and 100:20:0, was prepared for P-dosed and P-restricted conditions, respectively. The nutrient stock solution was added to the feed water to enhance biofilm growth in the flow cell increasing the assimilable organic carbon concentration of the feed water by $250 \mu\text{g C}\cdot\text{L}^{-1}$ and $30 \mu\text{g C}\cdot\text{L}^{-1}$. Chemicals from Sigma Aldrich (Darmstadt, Germany) were purchased in analytical grade. The pH-value was set at 11 by the addition of sodium hydroxide, to restrict bacterial growth in the nutrient stock solution. The feed water flow rate was high (17.0 L h^{-1}) compared to the dosing flow rate of the nutrient solution (0.03 L h^{-1}). Consequently, the high pH-value of the nutrient solution did not affect the feed water pH of 7.8 (Farhat et al., 2019). Two fully independent membrane fouling simulators ($N = 2$) were run for each set of experiments, and the figures show the average and standard deviation.

2.3. Phosphorus concentration in the feed water

To quantify low concentrations of ortho-phosphate a low detection auto analyzer using a colorimetric based method was applied (SEAL AutoAnalyser 3 HR Seal Analytical, Germany) following the proposed protocol by Murphy and Riley (1962). The phosphorus concentration reported in this study was calculated from the obtained ortho-phosphate concentration. Triplicate feed water samples were processed. For the P-restricted water, the phosphorus concentration was below the detection limit using the colorimetric auto analyzer method ($\leq 0.3 \mu\text{g P}\cdot\text{L}^{-1}$). For the P-dosed water, the measured phosphorus concentrations (26.0 and $3.5 \mu\text{g P}\cdot\text{L}^{-1}$) were in good agreement with the dosed phosphorus concentrations ($25.0 \mu\text{g P}\cdot\text{L}^{-1}$ and $3.0 \mu\text{g P}\cdot\text{L}^{-1}$, respectively).

2.4. Fouling monitoring

2.4.1. System performance parameters: feed channel pressure drop

Two sets of experiments (one for each carbon concentration) consisting of four membrane fouling simulators were run in parallel. Fouling development was monitored by measuring the feed channel pressure drop over the length of the flow cell. The average initial pressure drop registered in each MFS was 27 ± 4 mbar. For both carbon concentrations, experiments stopped once a feed channel pressure drop increase of 150 mbar reached. Pressure drop was selected as the membrane performance indicator as reverse osmosis biofouling is in practice predominantly a feed spacer channel problem (Vrouwenvelder et al., 2009). At full-scale RO installations operated for long periods (up to 10 years) with the same membrane modules fed with water containing very low

biodegradable nutrient (AOC) concentrations, the cleaning cycle was governed by the feed channel pressure drop increase (Beyer et al., 2014; Vrouwenvelder et al., 2008). Biofouling due to biodegradable nutrients in the feed water affects the membrane performance decline in a temporal sequence: first, the feed channel pressure drop is increased, then at a later moment and to a lesser extent the flux decline followed by increased salt passage (Siebdrath et al., 2019).

2.4.2. Biomass quantification

Membrane autopsies at the end of the experiment were carried out by retrieving membrane and feed spacer coupons of $4 \times 4 \text{ cm}^2$ from the MFS to quantify and characterize the accumulated fouling. Sheets of membrane and spacer were analyzed for total organic carbon (TOC) and adenosine triphosphate (ATP). The feed water surface area of the membrane is $4 \times 4 \text{ cm}^2$. The total surface area of the feed spacer is depending on the spacer geometry and thickness, approximately similar to the surface area of the membrane sheet area facing the feed water.

The sections of the membranes and spacer (8 cm^2 each) were placed in a capped tube in 40 mL sterile tap water for ATP analysis or ultrapure water for TOC analysis. To determine the amount of biomass, the tubes with the membrane and spacer coupons were placed in an ultrasonic water bath (Branson, 5510MTH, output 135 W, 40 kHz). Low energy sonic treatment (2 min) followed by mixing on a vortex (few seconds) was repeated two times. When the liquid was visually not homogeneous or when all biomass was not removed from the coupons, additional time-interval treatments were applied with a sonifier probe (Q700 Qsonica sonicator, USA) for 1–2 min (sample kept on ice) until the liquid was homogenous. Water collected from the tubes was used to determine the biomass parameters ATP and TOC. ATP was measured using a luminometer (Celsis Advance, Charles River Laboratories, Inc., USA) and TOC was measured with a Total Organic Carbon analyzer TOC-VCPH (Shimadzu, Japan) equipped with a high-sensitive catalyst (High sense TC catalyst; Shimadzu, Japan). The TOC concentration for each sample was the average of the three measurements. Samples were measured in duplicates. To prepare a calibration curve a stock solution of potassium hydrogen phthalate (TOC-standard solution ICC-033-5, ULTRA scientific, USA) was diluted with ultrapure water to obtain solutions with carbon concentrations between 0 and $10 \text{ mg L}^{-1} \text{ C}$. The detection limit of the method was about $0.1 \text{ mg L}^{-1} \text{ C}$.

2.4.3. Flow cytometry

Flow cytometry was used to measure the bacterial total cell counts (TCC) in the biofilm according to the protocol reported by Neu et al. (2019) in order to compare the bacterial total cell concentration between biofilms. In brief, a $4 \times 2 \text{ cm}^2$ coupon of biofouled membrane and spacer was placed in a capped tub in 40 mL ultrapure water, followed by 2 min of vortexing to separate the biomass from the membrane and spacer. Samples ($500 \mu\text{L}$) were preheated to $35 \text{ }^\circ\text{C}$ for 10 min, stained with $10 \mu\text{L mL}^{-1}$ SYBR Green I (Molecular Probes, Eugene, OR, USA), then incubated in the dark at $35 \text{ }^\circ\text{C}$ for 10 min. Measurements were performed using a BD Accuri C6 flow cytometer (BD Accuri Cytometers, Belgium) equipped with

Table 1
Experimental conditions to study the impact of phosphorus limitation on biofilm development.

Dosed carbon concentration ($\mu\text{g C}\cdot\text{L}^{-1}$)	Dosed phosphorus concentration ($\mu\text{g P}\cdot\text{L}^{-1}$)	Code	Nutrient C:N:P ratio	Measured phosphorus concentration ($\mu\text{g P}\cdot\text{L}^{-1}$)
250	25.0	P-dosed	100:20:10	26.0
	0.0	P-restricted	100:20:0	≤ 0.3
30	3.0	P-dosed	100:20:10	3.5
	0.0	P-restricted	100:20:0	≤ 0.3

a 50 mW laser having a fixed emission wavelength of 488 nm. Fluorescence intensity was collected at FL1 = 533 ± 30 nm, FL3 > 670 nm, sideward and forward scattered light intensities were obtained as well. All data were processed with the BD Accuri CFlow® software, and electronic gating was used to select SYBR green labeled signals for quantifying total bacterial cell count following the procedure described by Hammes and Egli (2005).

2.4.4. Extraction and quantification of extracellular polymeric substances (EPS)

For EPS analysis a 4×4 cm² coupon of biofouled membrane and spacer was placed into 10 mL phosphate-buffered saline solution (PBS), followed by 2 min of vortexing and 5 min of sonication to separate the biomass from the membranes. The EPS was extracted following the formaldehyde–NaOH method established by Liu and Fang (2002) and quantified by measuring carbohydrates (sulfuric acid phenol method) and proteins (BSA). In brief, the EPS suspended in 10 mL PBS was treated using 0.06 mL formaldehyde (36.5%; Sigma-Aldrich, MO, USA) at 4 °C for 1 h and incubated with 4 mL 1 N NaOH at 4 °C for 3 h. After treatment, the samples were centrifuged for 20 min at 20000×g. The supernatant was filtered through a 0.2 μm pore-sized membrane and dialyzed using a 3500 Da dialysis membrane (Thermo Fisher Scientific, USA) for 24 h. The dialyzed samples were lyophilized for 48 h and re-suspended in 10 mL of MQ water. The carbohydrates were measured following the sulfuric acid phenol method (Masuko et al., 2005). In brief, 200 μL of the sample was mixed with 600 μL sulfuric acid and 120 μL 5% phenol. The samples were then incubated at 90 °C for 5 min and left to cool down. The absorbance at 490 nm was measured using a Spectra A max 340pc microplate reader (Molecular Devices, USA). The protein concentrations using bovine serum albumin (BSA) as a standard, were measured using a BCA protein assay kit (Thermo Scientific Inc., NH, USA) according to the manufacturer's guidelines.

2.4.5. Biofilm structural properties

2.4.5.1. Optical coherence tomography (OCT). OCT uses coherent light to capture A-scans of optical scattering media such as biofilms. Consecutive A-scans provide a cross-sectional view in two dimensions (2D) of the biofilm structure (B-scan). B-scans are combined to volumetric representations, consequently 3D structures are capable to be visualized in seconds. *In-situ* imaging of the biofilm in the flow channel was performed using a spectral-domain Optical Coherence Tomography (Thorlabs Ganymede OCT System) with a central light source wavelength of 930 nm. The refractive index was 1.33. The OCT fitted with a $5 \times$ telecentric scan lens (Thorlabs LSM03BB), provided a maximum scan area of 100 mm². The OCT engine is configured to provide high-resolution images at a 36 kHz A-scan rate. Twenty images were taken at twenty randomized coordinates across the entire membrane fouling simulator (B-scan, x-z direction) consisting of a length of 5.00 mm and a physical depth of 1 mm with a pixel size in the x-direction of 6.00 μm and a z-direction of 2.13 μm, were taken and used for quantification purposes. Image processing details with respect to calculated biofilm porosity and area occupied by biofilm in the examined section of the flow channel, were quantified using the software developed in Matlab® (MathWorks, Natick, US) as can be found in previous publications (Derlon et al., 2012; Desmond et al., 2018). Image analysis consisted of i) detecting the membrane, spacer and biofilm interface with an intensity gradient analysis at the beginning and the end of the experiment; ii) automatic thresholding of the biofilm for pixels above 20 dB; this threshold was selected after analyzing more than 200 images studied in twenty independent membrane fouling simulators, and then excluding the membrane and spacer taken at time zero; iii)

calculation of the area occupied by biofilm in the cross-section of the flow channel, and the biofilm porosity.

2.4.5.2. Area occupied by biofilm in the cross-section of the flow channel. The membrane and feed spacer area occupied by biofilm in the cross-section of the flow channel was calculated based on the pixel area covered by biofilm from each OCT image. Twenty random images were taken at the inlet and outlet location of each MFS.

2.4.5.3. Biofilm calculated porosity. The biofilm porosity is the ratio between the total void area in the biofilm and the biofilm total area (Blauert et al., 2015). In this study, we considered biofilm voids as areas with an intensity below 20 dB in the two-dimensional OCT scan. The area of the biofilm consisted of the pixels with an intensity higher than 20 dB, excluding pixels from the membrane and spacer. However, it has to be emphasized that the resolution of the OCT is limited to 6 μm; thus, only voids larger than the 6 μm are considered. Therefore, the calculated biofilm porosity in this study refers only to the voids of the biofilm structure detected by the OCT (>6 μm).

$$\varphi_b = \frac{1}{N} \sum_1^N \frac{A_{voids}}{A_{biofilm}} \quad (1)$$

where φ_b is the biofilm calculated porosity, A_{voids} and $A_{biofilm}$ [m²] are the areas of the voids and the biofilm respectively, and N is the number of measurements.

3. Results

3.1. High assimilable organic carbon concentration (250 μg C·L⁻¹)

The MFSs that were operated under phosphorus-restricted (P-restricted), and phosphorus-dosed (P-dosed) conditions were stopped once a feed channel pressure drop increase of 150 mbar was reached (Fig. 1). For a high assimilable organic carbon content of 250 μg C·L⁻¹, P-restricted biofilms caused a faster feed channel pressure drop increase than the P-dosed biofilms.

The TOC content was more than two times lower (Fig. 2A) under P-restricted conditions compared to when phosphorus was dosed (0.03 mg cm⁻² versus 0.07 mg cm⁻², respectively). The ATP concentration (Fig. 2B) and total bacterial cell count (TCC) had the same trend for P-restricted and P-dosed conditions (Fig. 2C). The ATP concentration was about 19 times lower under P-restricted conditions compared to when phosphorus was dosed

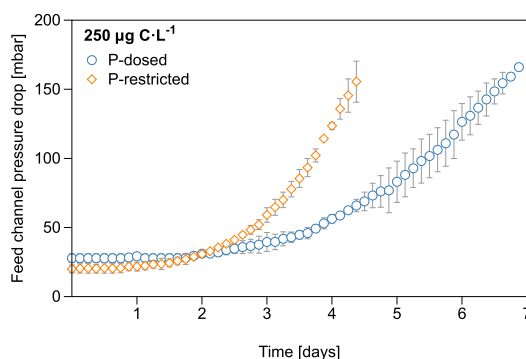


Fig. 1. Feed channel pressure drop [mbar] in time over the MFS for the P-restricted (<0.3 μg P·L⁻¹) and the P-dosed (25 μg P·L⁻¹) feed water conditions for a dosed high assimilable organic carbon concentration of 250 μg C·L⁻¹. Fully independent duplicate experiments are shown. The MFSs were stopped and sampled for biofilm analysis once a feed channel pressure drop increase of 150 mbar was reached.

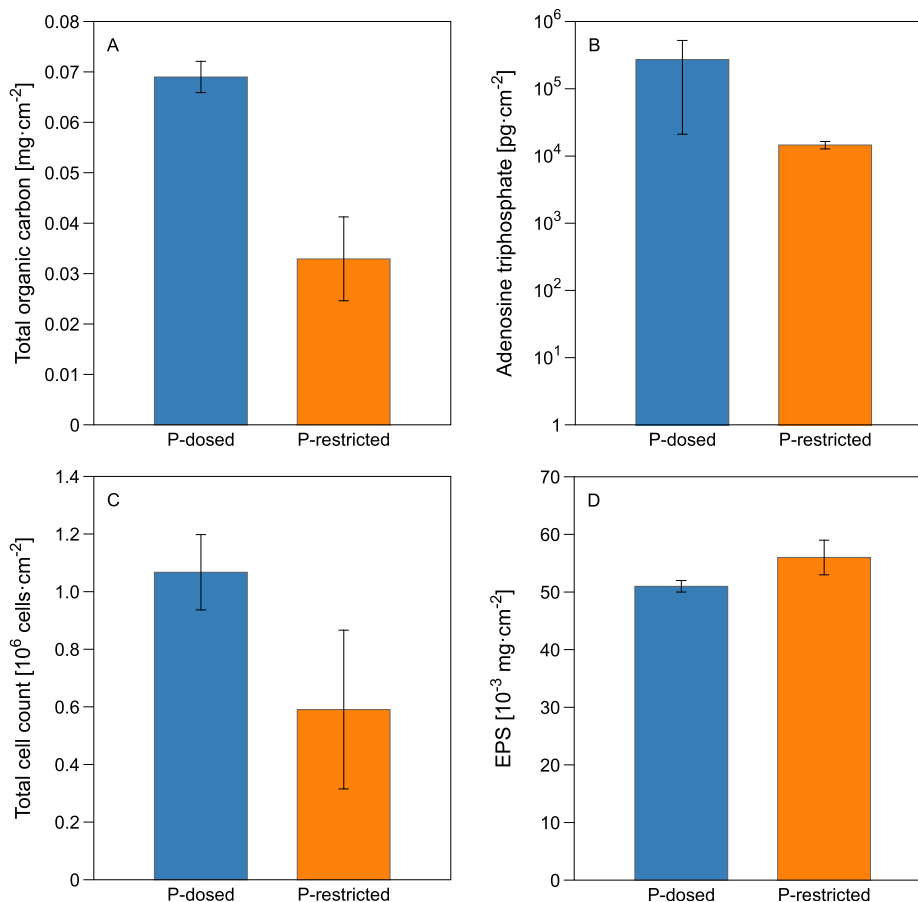


Fig. 2. (A) Total organic carbon (TOC), (B) Adenosine triphosphate (ATP), (C) Total cell count (TCC), and (D) EPS for the P-dosed ($25 \mu\text{g P}\cdot\text{L}^{-1}$) and P-restricted ($<0.3 \mu\text{g P}\cdot\text{L}^{-1}$) biofilms for a dosed assimilable organic carbon concentration of $250 \mu\text{g C}\cdot\text{L}^{-1}$. The area (cm^2) referred here is the top view surface area (xy direction). Fully independent duplicate experiments are shown. All experiments were stopped and sampled for biofilm analysis once a normalized feed channel pressure drop increase of 150 mbar was reached.

($1.45 \times 10^4 \text{ pg cm}^{-2}$ versus $2.71 \times 10^5 \text{ pg cm}^{-2}$, respectively). The TCC for the P-restricted biofilm was only two times lower for the P-dosed biofilm ($0.59 \times 10^6 \text{ cells}\cdot\text{cm}^{-2}$ versus $1.07 \times 10^6 \text{ cells}\cdot\text{cm}^{-2}$, respectively). The EPS content for the P-restricted biofilm was higher than that for the P-dosed biofilm ($56 \times 10^{-3} \text{ mg cm}^{-2}$ versus $51 \times 10^{-3} \text{ mg cm}^{-2}$, respectively, Fig. 2D). In summary, P-restricted conditions limited bacterial growth (lower values of ATP, TOC, TCC) but produced more EPS compared to P-dosed conditions, causing a faster increase in the feed channel pressure drop.

Based on two-dimensional OCT images, the area occupied by biofilm and the porosity of the biofilm in the examined section of the flow channel are calculated. Compared to P-dosed biofilms, P-restricted biofilm had three times more area occupied by biofilm ($5.2 \times 10^{-2} \text{ mm}^2$ versus $1.7 \times 10^{-2} \text{ mm}^2$, respectively, Fig. 3A). P-restricted biofilms were three times more porous compared to P-dosed biofilms (0.65 compared to 0.18, respectively, Fig. 3B). Fig. 3C shows the two-dimensional OCT images. Compared to the P-restricted biofilm, the P-dosed biofilm occupied a smaller surface area in the flow channel with high intensity pixels surrounding the spacer. A smaller coverage area with higher concentrations of TOC, ATP, and TCC can signal to the formation of a denser more compact biofilm. The P-restricted biofilm occupied a larger area in the flow channel with lower concentrations of TOC, ATP, and TCC. The intensity profile around the spacer showed areas of lower intensity with much bigger areas with very low intensity considered as voids. The higher calculated porosity of the formed biofilm correlates with the lower biomass amount (lower values of ATP, TOC and TCC). P-

restricted biofilm disrupted more the cross-flow in the feed channel and therefore caused the faster increase of the feed channel pressure drop, compared to biofilms grown under P-dosed conditions.

3.2. Low assimilable organic carbon concentration ($30 \mu\text{g C}\cdot\text{L}^{-1}$)

The second set of experiments was performed to analyze the effect of limiting the assimilable organic carbon to $30 \mu\text{g C}\cdot\text{L}^{-1}$ at phosphorus concentration of $3 \mu\text{g P}\cdot\text{L}^{-1}$ and $<0.3 \mu\text{g P}\cdot\text{L}^{-1}$ in the feed water. Contrary to the $250 \mu\text{g C}\cdot\text{L}^{-1}$ experiment, the P-restricted biofilm caused a slower feed channel pressure drop increase than the P-dosed biofilm (Fig. 4). The P-restricted biofilm had a lower TOC concentration compared to the P-dosed biofilm (0.01 versus 0.02 mg cm^{-2} , respectively, Fig. 5A). The ATP concentration was lower under P-restricted conditions compared to when phosphorus was dosed ($3.30 \times 10^3 \text{ pg cm}^{-2}$ versus $7.30 \times 10^3 \text{ pg cm}^{-2}$, respectively, Fig. 5B). Once again, the P-restricted biofilm had a higher EPS content than the P-dosed biofilm ($20.00 \times 10^{-3} \text{ mg cm}^{-2}$ versus $12.00 \times 10^{-3} \text{ mg cm}^{-2}$, respectively, Fig. 5C). Therefore, results in TOC, ATP, and the EPS for the biofilm grown under $30 \mu\text{g C}\cdot\text{L}^{-1}$ showed the same trends as for the biofilm grown under $250 \mu\text{g C}\cdot\text{L}^{-1}$.

Fig. 6 shows the area occupied by the biofilm in the flow channel. The P-restricted and P-dosed biofilms occupied almost the same area in the flow channel at the end of the experiment. The P-restricted biofilm was significantly ($P < 0.05$) more porous in

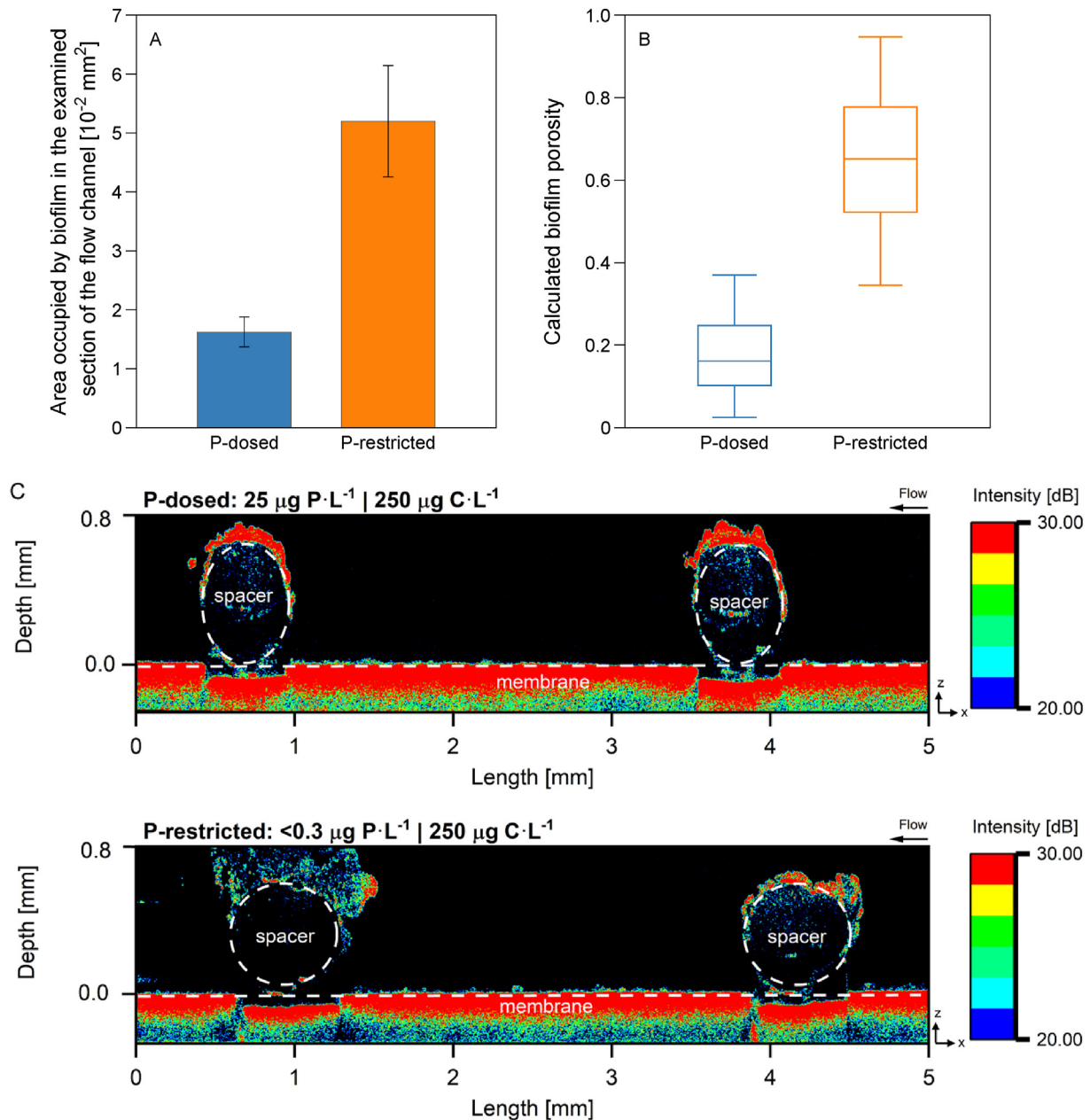


Fig. 3. (A) Area occupied by biofilm in the examined section of the flow channel (mm^2), (B) calculated biofilm porosity and (C) two-dimensional OCT images with intensity profile of the biofilms developing on the membrane under P-restricted ($<0.3 \mu\text{g P}\cdot\text{L}^{-1}$) and P-dosed ($25 \mu\text{g P}\cdot\text{L}^{-1}$) conditions for a dosed assimilable organic carbon concentration of $250 \mu\text{g C}\cdot\text{L}^{-1}$ ($N = 20$). The OCT signal intensity was used to describe biofilm properties, with higher intensity resulting from a more light-scattering biofilm. Note that the thickness of the spacer in the OCT images does not correspond necessarily to 34 mil, because the thickness of the spacer's filaments is irregular, as shown in previous studies (Bucs et al., 2015; Haaksmann et al., 2017). All experiments were stopped and sampled for biofilm analysis once a normalized feed channel pressure drop increase of 150 mbar was reached. The arrows indicate the crossflow direction.

agreement with the biofilm grown under $250 \mu\text{g C}\cdot\text{L}^{-1}$. The biofilm calculated porosity for P-restricted and P-dosed conditions was 0.53 versus 0.27, respectively (Fig. 6B). Two-dimensional OCT images showed a higher intensity for biofilms grown under P-dosed conditions compared to the P-restricted biofilm, which shows areas of lower intensity around the spacer, with higher calculated biofilm porosity (Fig. 6C).

Table 2 summarizes the results of all experiments. The opposite trend of the feed channel pressure drop increase for biofilms grown under $250 \mu\text{g C}\cdot\text{L}^{-1}$ and $30 \mu\text{g C}\cdot\text{L}^{-1}$, while restricting the phosphorus content, can be explained by two factors. The first factor is the difference at which the active biomass is producing EPS per day.

For the biofilm grown at $250 \mu\text{g C}\cdot\text{L}^{-1}$, P-restricted biofilm produced 70% more EPS per day compared to the P-dosed biofilm. Whereas, the P-restricted biofilm grown at $30 \mu\text{g C}\cdot\text{L}^{-1}$ produced only 25% more EPS per day than the P-dosed biofilm. The second factor is related to the difference in biofilm spatial distribution in the flow channel under different assimilable organic carbon concentrations. When phosphorus was restricted but sufficient amount of carbon was available ($250 \mu\text{g C}\cdot\text{L}^{-1}$), the biofilm that developed occupied a higher surface area in the flow channel per day (+300%) compared to the P-dosed biofilm, which resulted in an accelerated increase in the feed channel pressure drop. On the contrary, for a lower assimilable organic carbon content

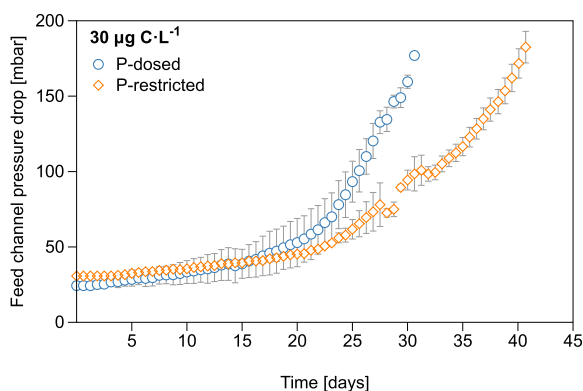


Fig. 4. Feed channel pressure drop [mbar] in time over the MFS for the P-restricted ($<0.3 \mu\text{g P}\cdot\text{L}^{-1}$) and the P-dosed ($3 \mu\text{g P}\cdot\text{L}^{-1}$) feed water conditions for a dosed assimilable organic carbon concentration of $30 \mu\text{g C}\cdot\text{L}^{-1}$. Fully independent duplicate experiments are shown. The MFSs were stopped and sampled for biofilm analysis once a feed channel pressure drop increase of 150 mbar was reached.

($30 \mu\text{g C}\cdot\text{L}^{-1}$), the P-restricted biofilm covered 33% less surface area per day in the flow channel, compared to the P-dosed biofilm, resulting in a slower increase in the feed channel pressure drop.

4. Discussion

4.1. Phosphorus limitation restricts microbial growth but increases EPS secretion in abundance of assimilable organic carbon

Previous studies on phosphorus limiting conditions demonstrated an excessive production of extracellular polymeric substances (Desmond et al., 2018), but lower bacterial growth, characterized by the active biomass (ATP) and total bacterial cell count (TCC) (Kim et al., 2014; Vrouwenvelder et al., 2010). Kim et al. (2014) demonstrated that the total bacterial cell count was reduced when decreasing the phosphorus concentration in the feed water of a forward osmosis membrane system. The objective of this study was to compare the effect of restricting phosphorus in the feed water at two assimilable organic carbon concentrations (250 and $30 \mu\text{g C}\cdot\text{L}^{-1}$) on membrane performance and biomass activity in a reverse osmosis membrane system. In agreement with previous studies, P-restricted conditions limited bacterial growth (lower values of ATP and TCC) but increased EPS secretion compared to P-dosed conditions at both carbon concentrations. This EPS production under P-restricted conditions affected the biofilm structural

properties, and thus the system performance (feed channel pressure drop increase) differently depending on the assimilable organic carbon concentration (Fig. 7). The observed faster pressure drop increase for P-restricted conditions when dosing $250 \mu\text{g C}\cdot\text{L}^{-1}$ was a result of the larger area occupied by a more porous biofilm in the flow channel (Fig. 3).

This study used tapwater as feedwater, but it is expected that the observations obtained in this study for tap water can be applied to SWRO. The yield of bacterial growth is the same for fresh, tap and seawater with the same biodegradable nutrient content (Farhat et al., 2018). Bacterial cells in a biofilm typically make up a very small fraction (less than a half percent) of the overall biofilm volume and therefore do not hamper the water flow through the biofilm significantly (Dreszer et al., 2013). The hydraulic biofilm resistance is mainly attributed to the (amount and density of) extracellular polymeric substances (EPS) and not to the bacterial cells (Dreszer et al., 2013).

The importance of EPS and its composition on membrane performance decline and cleanability has been demonstrated (Flemming and Wingender, 2010; Flemming, 2020; Jafari et al., 2020). Therefore, it is vital to note that when the bacteria are different in seawater, the EPS produced by these bacteria could be different. Future biofilm studies comparing biofouling development in membrane systems fed with fresh and with seawater will include the assessment of the bacterial community composition (and the EPS structure and composition) of the biofilm and the feed water.

4.2. Nutrient limitation influences biofilm morphology and spatial distribution

Analytical quantification of ATP, TOC, TCC, and EPS give an estimate of the biomass concentration on the membrane and the spacer. However, these parameters do not show the spatial distribution of the biofilm in the MFS and the biofilm structure. Feed channel pressure drop measurements are based on the resistance that water experiences when passing through the flow channel (Bucs et al., 2016; Drescher et al., 2013). This study showed that under high assimilable organic carbon concentration, even less biomass (ATP, TCC, and TOC) can have a higher impact on the feed channel pressure drop (Fig. 1). Therefore, besides the amount of biomass, biofilm structural properties such as porosity and the location in the flow channel, play an essential role on the effect of membrane performance parameters (Fortunato et al., 2017).

In this study, the greater influence of the P-restricted biofilm on the feed channel pressure drop when dosing $250 \mu\text{g C}\cdot\text{L}^{-1}$

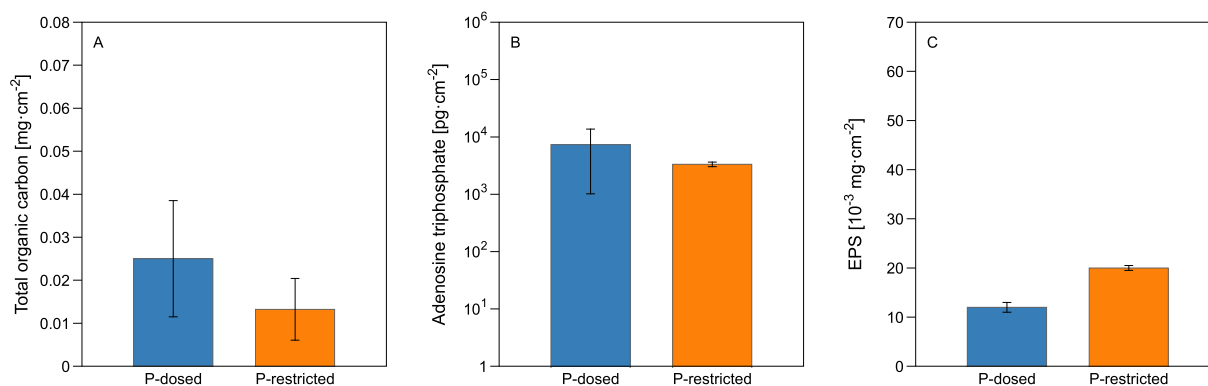


Fig. 5. (A) Total organic carbon (TOC), (B) Adenosine triphosphate (ATP), and (C) EPS for the P-dosed ($3 \mu\text{g P}\cdot\text{L}^{-1}$) and P-restricted ($<0.3 \mu\text{g P}\cdot\text{L}^{-1}$) biofilms for a dosed assimilable organic carbon concentration of $30 \mu\text{g C}\cdot\text{L}^{-1}$. The area (cm^2) referred here is the top view surface area (xy direction). Fully independent duplicate experiments are shown. All experiments were stopped and sampled for biofilm analysis once a normalized feed channel pressure drop increase of 150 mbar was reached.

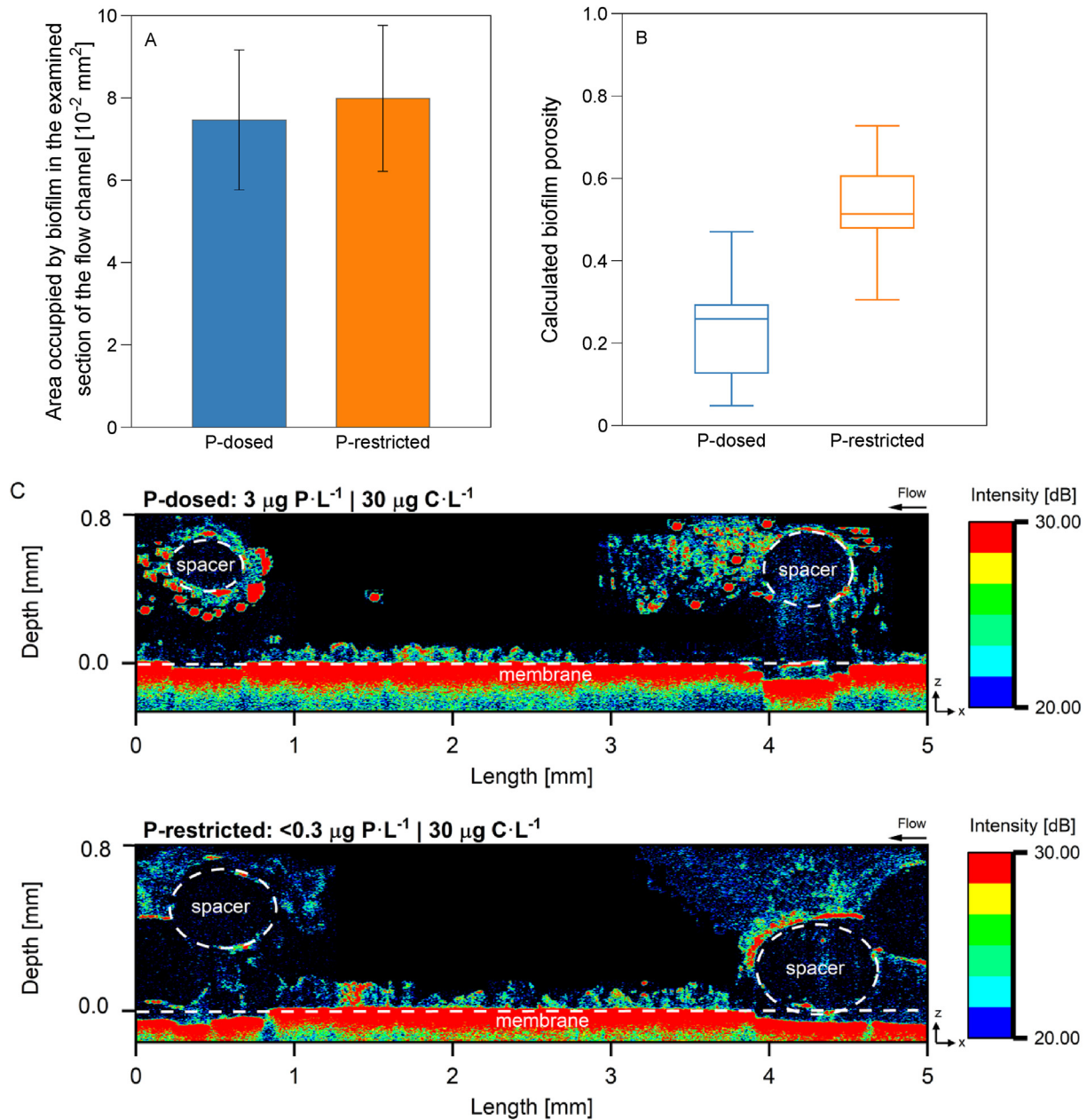


Fig. 6. (A) Area occupied by biofilm in the examined section of the flow channel (mm²), (B) calculated biofilm porosity and (C) two-dimensional OCT images with intensity profile of the biofilms developing on the membrane under P-restricted (<math><0.3 \mu\text{g P}\cdot\text{L}^{-1}</math>) and P-dosed ($3 \mu\text{g P}\cdot\text{L}^{-1}$) conditions for a dosed assimilable organic carbon concentration of $30 \mu\text{g C}\cdot\text{L}^{-1}$ (N = 20). The OCT signal intensity was used to describe biofilm properties, with higher intensity resulting from a more light-scattering biofilm. Note that the thickness of the spacer in the OCT images does not correspond necessarily to 34 mil, because the thickness of the spacer's filaments is irregular, as shown in previous studies (Bucs et al., 2015; Haaksman et al., 2017). All experiments were stopped and sampled for biofilm analysis once a normalized feed channel pressure drop increase of 150 mbar was reached. The arrows indicate the cross-flow direction.

Table 2

Summary of the results for the biofilms grown at two carbon concentrations $250 \mu\text{g C}\cdot\text{L}^{-1}$ and $30 \mu\text{g C}\cdot\text{L}^{-1}$.

Carbon concentration [$\mu\text{g C}\cdot\text{L}^{-1}$]	250		30	
Phosphorus concentration [$\mu\text{g P}\cdot\text{L}^{-1}$]	<math><0.3</math>	25	<math><0.3</math>	3
Time to reach 150 mbar [days]	4.2	6.5	40	28
TOC [$\text{mg}\cdot\text{cm}^{-2}$]	0.03	0.07	0.01	0.02
ATP [$\times 10^3 \text{pg cm}^{-2}$]	14	271	3	7
EPS [$\times 10^{-3} \text{mg cm}^{-2}$]	56	51	20	12
EPS/day [$\times 10^{-3} \text{mg cm}^{-2}\cdot\text{day}^{-1}$]	13.3	7.8	0.5	0.4
Covered area by the biofilm in the xz direction [$\times 10^{-2} \text{mm}^2$]	5.2	1.7	8	7.5
Covered area by the biofilm/day in the xz direction [$\times 10^{-2} \text{mm}^2\cdot\text{day}^{-1}$]	1.2	0.3	0.2	0.3
Biomass volume in the xyz direction/area [$\text{mm}^3\cdot\text{cm}^{-2}$]	1.0	0.3	1.6	1.5
Biofilm calculated porosity	0.65	0.18	0.53	0.27

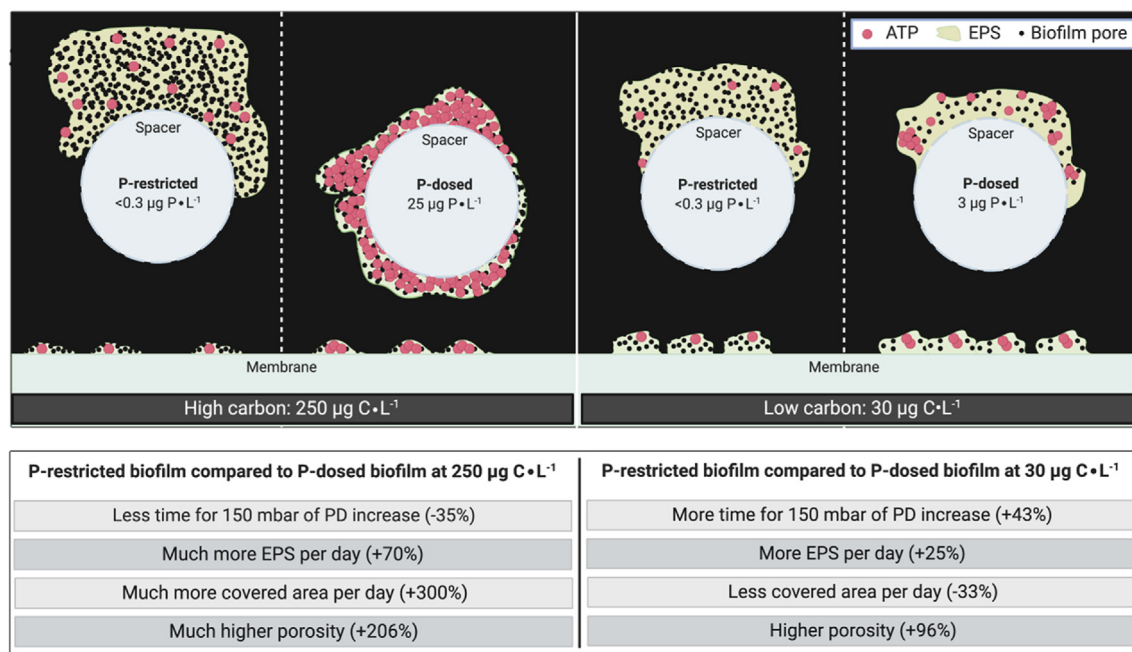


Fig. 7. Biofilm schematic for high ($250 \mu\text{g C}\cdot\text{L}^{-1}$) and low ($30 \mu\text{g C}\cdot\text{L}^{-1}$) carbon concentrations, at low phosphorus concentration (P-restricted $<0.3 \mu\text{g P}\cdot\text{L}^{-1}$) in the feed water.

compared with the $30 \mu\text{g C}\cdot\text{L}^{-1}$, can be explained by the biofilm metabolic and structural responses to nutrient restriction. OCT images showed that for a high assimilable organic carbon concentration, three times more area was occupied by the biofilm in the flow channel under restricted phosphorus conditions compared to P-dosed condition (Fig. 3A). Studies on nutrient limiting conditions demonstrate changes in bacterial physiology, triggering cell elongation, filamentous growth which resulted in the formation of a dispersed biofilm floc (Ericsson and Eriksson, 1988; Romano et al., 2015; Seviour et al., 2019). The uniform distribution of biofilm over the whole flow cell under limitation conditions and its effect on performance should not be neglected. The change in bacterial physiology combined with the higher EPS production resulted in a more porous biofilm covering a larger area in the flow channel, restricting the water flow.

In the case of a low assimilable organic carbon content and P-dosed conditions, bacteria at the beginning of the experiment did not have any nutrient limitation. Note that clusters of dense biofilm accumulate close to the spacer (Fig. 6C), similar of how the biofilm developed under high assimilable organic content and P-dosed conditions. As the biofilm continues to develop, carbon limitation occurs, biofilm then starts to spread to maximize nutrient intake, linked to the higher rate of pressure drop increase under this condition. For the biofilm grown at low assimilable organic carbon content and P-restricted conditions, the developed biofilm structure signified the occurrence of dual nutrient limitation; definitely, with one substrate being the limiting substrate at one period in time, starting with P-limitation followed by C-limitation. P-restricted biofilm started to spread to maximize nutrient intake, however the EPS production per day is not as fast as in the presence of abundant assimilable organic carbon content (+25% versus +70%, respectively). The covered area by the P-restricted biofilm in the flow channel is 33% lower compared to the P-dosed conditions, which explains the slower pressure drop increase (Table 2). An important fact to note is that according to this study, phosphorus restriction combined with carbon restriction delayed biofilm formation, extending system performance by 43% compared to biofilms grown under P-dosed conditions. Moreover,

additional experiments run in duplicates under different operating conditions (e.g. different cross-flow velocity and ended at different values of pressure drop increase, data not included in this paper) supported the conclusions of this study.

Results from this study highlight that the conventional biomass quantification parameters (ATP, TOC, TCC and EPS) did not correlate with the pressure drop increase and cannot aid in predicting the system performance decline. The two parameters combined together that correlated the most with the pressure drop increase where the: (i) area occupied by the biofilm in the flow channel and (ii) biofilm spatial distribution (spacer/membrane).

4.3. Carbon concentration determines the effectiveness of phosphorus limitation as a biofouling control strategy

Restricting the phosphorous concentration resulted in a varying impact on feed channel pressure drop depending on the concentration of assimilable organic carbon that was dosed (Fig. 7). Limiting only the phosphorous content while dosing a relatively higher carbon concentration produced a biofilm that lead to a faster pressure drop. A strategy based on nutrient limitation should focus on the appropriate selection of the nutrient ratio in the feed water. The amount of nutrient converted by bacterial cells to EPS depends on the composition of the growth medium. A growth medium containing a high ratio of carbon with a limited phosphate, enhanced polysaccharide production as shown in (Miqueleto et al., 2010). In this study, for the high carbon concentration ($250 \mu\text{g C}\cdot\text{L}^{-1}$) even at a deficient phosphorus concentration in the feed water ($\leq 0.3 \mu\text{g P}\cdot\text{L}^{-1}$), the C:P ratio was 833:1, while for the low carbon concentration ($30 \mu\text{g C}\cdot\text{L}^{-1}$), the C:P ratio was 100:1. When the C:P ratio is high, the bacteria utilize the excess carbon for EPS production rather than cell growth, since there is insufficient phosphorus for ATP synthesis (Miqueleto et al., 2010). Particular attention should be given to the carbon concentration in feedwater because limiting phosphorus without knowing the amount of carbon concentration, may result in a negative impact in the feed channel pressure drop increase compared to a non-limiting phosphorus condition. Depending on the available carbon

concentration, phosphate limitation can be a strategy to prevent biofouling, requiring the elimination of phosphate/phosphorous based anticalant dosage in pretreatment (Sweity et al., 2013). The presence of both very low concentrations of phosphate and biodegradable substrate in the feed water of a full-scale RO installation lead to low biofilm concentrations in the lead and outlet modules of the installation compared to most installations studied (Vrouwenvelder et al., 2008), indicating that combined restriction of phosphate and biodegradable nutrients limited the decline in membrane performance indicators. Slightly higher biofilm accumulation in the membrane module at the outlet side of the RO installation was observed under these low nutrient conditions (Vrouwenvelder et al., 2010, 2008). Radu et al. (2012) clearly illustrated in numeral simulations how the membrane rejected biodegradable substrates accumulates at the membrane surface due to concentration polarization. With an increased biofilm thickness, however, the overall substrate consumption rate dominates the substrate accumulation due to polarization. Therefore, the accumulation of rejected biodegradable substrate could only accelerate in a limited extent the biofilm growth (Radu et al., 2012). Further studies are recommended on concentration polarization of phosphate, salt and biodegradable nutrients in relation to biofouling and scaling.

The difficulty of restricting phosphorous makes carbon limitation a more attractive and cost-effective approach for biofouling control in seawater. As shown in this study, even a minute amount of phosphorus in the feed water, at low carbon concentration, although delayed biofouling it did not completely eliminate its occurrence. On the contrary, regardless of the phosphorus concentration, a low assimilable organic carbon content delayed the membrane performance decline (pressure drop increase) significantly, compared to high carbon content.

4.4. Future research

Quantification of very low phosphorus concentrations in water remains a challenge. The principal obstacles are: (i) the limited available techniques to remove phosphorus (Kumar et al., 2019; Sevcenco et al., 2015; Shang et al., 2014b, 2014a) and (ii) the absence of available detection methods to allow reliable quantification of very low concentrations $\leq 0.3 \mu\text{g P}\cdot\text{L}^{-1}$ to validate the efficiency of the removal techniques. Results from this study emphasize the need for a reliable quantification method for determining phosphorus at concentrations lower than $0.3 \mu\text{g P}\cdot\text{L}^{-1}$. Ultra-trace phosphorus quantification techniques are needed to show at which P-concentration phosphorus limitation occurs, causing no biofilm development. In order to better understand phosphorus restriction and its effect on membrane performance, further studies should focus on: (i) analyzing the effect of permeation and concentration polarization under nutrient limitation conditions, (ii) analyzing the microbial community composition in the biofilm to determine bacterial community that can grow under phosphorus stressed conditions, (iii) understanding the carbon metabolic pathway for EPS production versus bacterial cell growth when phosphorus is restricted, and (iv) tuning the phosphorus concentration in the feed water to define the optimal effect on membrane performance and cleanability.

A future study to separately sample the accumulated material on the feed spacer and membrane and subsequently analyze the composition (TOC, cells, ATP, EPS and microbial community) is essential as well. Such study aids in determining whether e.g. hydraulics and permeate production affect the amount and composition of these biomass parameters and this research could include varying cross flow velocities and permeate fluxes.

5. Conclusions

The objective of this study was to analyze the effect of nutrient limitation on biofilm development and its impact on system performance. In this study we assessed the physical structure and chemical composition of the biofilms that developed under phosphorus-restricted conditions ($\leq 0.3 \mu\text{g P}\cdot\text{L}^{-1}$). Feed channel pressure drop was determined to understand the impact of the developed biofilm on system performance. The developed biofilm was analyzed once the feed channel pressure drop reached an increase of 150 mbar. The conclusions of this study can be summarized by:

- (i) Under P restricted conditions, for both supplemented assimilable organic carbon concentrations (250 and $30 \mu\text{g C}\cdot\text{L}^{-1}$) the biofilm that developed had less ATP, TCC, and TOC, but had higher EPS production, was more porous and occupied a larger area in the flow channel.
- (ii) A supplemented carbon concentration of $250 \mu\text{g C}\cdot\text{L}^{-1}$ and low feed water P-concentration ($\leq 0.3 \mu\text{g P}\cdot\text{L}^{-1}$) caused an *accelerated* feed channel pressure drop increase, explained by more EPS production and a larger area occupied by the biofilm in the cross-section of the flow channel, compared with biofilms that developed at a carbon concentration of $30 \mu\text{g C}\cdot\text{L}^{-1}$.
- (iii) The carbon concentration determines the effectiveness of phosphorus limitation, and therefore, the impact on the feed channel pressure drop.
- (iv) Limiting both carbon and phosphorus concentrations in the feed water proves to be a suitable approach in delaying biofilm formation and hence, lengthening the overall membrane system performance.

Declaration of competing interest

The authors declare that they have no known competing financial interests or personal relationships that could have appeared to influence the work reported in this paper.

Acknowledgments

The research reported in this publication was supported by funding from King Abdullah University of Science and Technology (KAUST).

References

- Abushaban, A., Salinas-Rodriguez, S.G., Dhakal, N., Schippers, J.C., Kennedy, M.D., 2019. Assessing pretreatment and seawater reverse osmosis performance using an ATP-based bacterial growth potential method. *Desalination* 467, 210–218.
- Allan, V.J.M., Callow, M.E., Macaskie, L.E., Paterson-Beedle, M., 2002. Effect of nutrient limitation on biofilm formation and phosphatase activity of a *Citrobacter* sp. *Microbiology* 148, 277–288.
- Beyer, F., Rietman, B.M., Zwijnenburg, A., van den Brink, P., Vrouwenvelder, J.S., Jarzembowska, M., Laurinonite, J., Stams, A.J.M., Plugge, C.M., 2014. Long-term performance and fouling analysis of full-scale direct nanofiltration (NF) installations treating anoxic groundwater. *J. Membr. Sci.* 468, 339–348.
- Blauert, F., Horn, H., Wagner, M., 2015. Time-resolved biofilm deformation measurements using optical coherence tomography. *Biotechnol. Bioeng.* 112, 1893–1905.
- Bucs, S., Farhat, N., Kruihof, J.C., Picioreanu, C., van Loosdrecht, M.C.M., Vrouwenvelder, J.S., 2018. Review on strategies for biofouling mitigation in spiral wound membrane systems. *Desalination* 434, 189–197.
- Bucs, S.S., Farhat, N., Siddiqui, A., Valladares Linares, R., Radu, A., Kruihof, J.C., Vrouwenvelder, J.S., 2016. Development of a setup to enable stable and accurate flow conditions for membrane biofouling studies. *Desalin. Water Treat.* 57, 12893–12901.
- Bucs, S.S., Valladares Linares, R., Marston, J.O., Radu, A.I., Vrouwenvelder, J.S., Picioreanu, C., 2015. Experimental and numerical characterization of the water flow in spacer-filled channels of spiral-wound membranes. *Water Res.* 87,

- 299–310.
- Burton, F., Tchobanoglous, G., Stensel, D., 2010. Wastewater engineering: treatment and reuse. In: Franklin Burton, George Tchobanoglous, H. David Stensel, fourth ed. Tata McGraw-Hill Education Pvt. Ltd. 0 9780070495395 Hardcover - BookVistas.
- Cade-Menun, B.J., Elkin, K.R., Liu, C.W., Bryant, R.B., Kleinman, P.J.A., Moore, P.A., 2018. Characterizing the phosphorus forms extracted from soil by the Mehlich III soil test. *Geochem. Trans.* 19, 1–17.
- Chandy, J.P., Angles, M.L., 2001. Determination of nutrients limiting biofilm formation and the subsequent impact on disinfectant decay. *Water Res.* 35, 2677–2682.
- Dabkowski, B., White, M., 2015. Understanding the different phosphorus tests. *Appl. Note Debunking Phosphorus Test* 1–4.
- Derlon, N., Peter-varbanets, M., Scheidegger, A., Pronk, W., Morgenroth, E., 2012. Predation influences the structure of biofilm developed on ultrafiltration membranes. *Water Res.* 46, 3323–3333.
- Desmond, P., Best, J.P., Morgenroth, E., Derlon, N., 2018. Linking composition of extracellular polymeric substances (EPS) to the physical structure and hydraulic resistance of membrane biofilms. *Water Res.* 132, 211–221.
- Drescher, K., Shen, Y., Bassler, B.L., Stone, H.A., 2013. Biofilm streamers cause catastrophic disruption of flow with consequences for environmental and medical systems. *Proc. Natl. Acad. Sci. U.S.A.* 110, 4345–4350.
- Dreszer, C., Vrouwenvelder, J.S., Paulitsch-Fuchs, A.H., Zwijnenburg, A., Kruihof, J.C., Flemming, H.C., 2013. Hydraulic resistance of biofilms. *J. Membr. Sci.* 429, 436–447.
- Elimelech, M., Phillip, W.A., 2011. The future of seawater desalination: energy, technology, and the environment. *Science* 333 (80), 712–717.
- Ericsson, B., Eriksson, L., 1988. Activated sludge characteristics in a phosphorus depleted environment. *Water Res.* 22 (2), 151–162.
- Farhat, N., Hammes, F., Prest, E., Vrouwenvelder, J., 2018. A uniform bacterial growth potential assay for different water types. *Water Res.* 142, 227–235.
- Farhat, N.M., Javier, L., Van Loosdrecht, M.C.M., Kruihof, J.C., Vrouwenvelder, J.S., 2019. Role of feed water biodegradable substrate concentration on biofouling: biofilm characteristics, membrane performance and cleanability. *Water Res.* 150, 1–11.
- Flemming, H.-C., 1997. Reverse osmosis membrane biofouling. *Exp. Therm. Fluid Sci.* 14, 382–391.
- Flemming, H., Wingender, J., 2010. The biofilm matrix. *Nat. Rev. Microbiol.* 8, 623–633.
- Flemming, H.C., 2020. Biofouling and me: my Stockholm syndrome with biofilms. *Water Res.* 173, 115576.
- Fortunato, L., Bucs, S., Linares, R.V., Cali, C., Vrouwenvelder, J.S., Leiknes, T.O., 2017. Spatially-resolved in-situ quantification of biofouling using optical coherence tomography (OCT) and 3D image analysis in a spacer filled channel. *J. Membr. Sci.* 524, 673–681.
- Greenlee, L.F., Lawler, D.F., Freeman, B.D., Marrot, B., Moulin, P., 2009. Reverse osmosis desalination: water sources, technology, and today's challenges. *Water Res.* 43, 2317–2348.
- Haaksman, V.A., Siddiqui, A., Schellenberg, C., Kidwell, J., Vrouwenvelder, J.S., Picioreanu, C., 2017. Characterization of feed channel spacer performance using geometries obtained by X-ray computed tomography. *J. Membr. Sci.* 522, 124–139.
- Hammes, F.A., Egli, T., 2005. New method for assimilable organic carbon determination using flow-cytometric enumeration and a natural microbial consortium as inoculum. *Environ. Sci. Technol.* 39, 3289–3294.
- Jacobson, J.D., Kennedy, M.D., Amy, G., Schippers, J.C., 2009. Phosphate limitation in reverse osmosis: an option to control biofouling? *Desalin. Water Treat.* 5, 198–206.
- Jafari, M., D'haese, A., Zlopasa, J., Cornelissen, E.R., Vrouwenvelder, J.S., Verbeke, K., Verliefde, A., van Loosdrecht, M.C.M., Picioreanu, C., 2020. A comparison between chemical cleaning efficiency in lab-scale and full-scale reverse osmosis membranes: role of extracellular polymeric substances (EPS). *J. Membr. Sci.* 609, 118189.
- Kim, C.M., Kim, S.J., Kim, L.H., Shin, M.S., Yu, H.W., Kim, I.S., 2014. Effects of phosphate limitation in feed water on biofouling in forward osmosis (FO) process. *Desalination* 349, 51–59.
- Kumar, P.S., Korving, L., van Loosdrecht, M.C.M., Witkamp, G.-J., 2019. Adsorption as a technology to achieve ultra-low concentrations of phosphate: research gaps and economic analysis. *Water Res. X* 4, 100029.
- Lehtola, M.J., Miettinen, I.T., Vartiainen, T., Myllykangas, T., Martikainen, P.J., 2001. Microbially available organic carbon, phosphorus, and microbial growth in ozonated drinking water. *Water Res.* 35, 1635–1640.
- Liu, H., Fang, H.H.P., 2002. Extraction of extracellular polymeric substances (EPS) of sludges. *J. Biotechnol.* 95, 249–256.
- Masuko, T., Minami, A., Iwasaki, N., Majima, T., Nishimura, S.-I., Lee, Y.C., 2005. Carbohydrate analysis by a phenol–sulfuric acid method in microplate format. *Anal. Biochem.* 339, 69–72.
- Matin, A., Khan, Z., Zaidi, S.M.J., Boyce, M.C., 2011. Biofouling in reverse osmosis membranes for seawater desalination: phenomena and prevention. *Desalination* 281, 1–16.
- Miettinen, I.T., Vartiainen, T., 1997. Phosphorus and bacterial growth in drinking water. *Appl. Environ. Microbiol.* 63, 3242–3245.
- Miqueleto, A.P., Dolosic, C.C., Pozzi, E., Foresti, E., Zaiat, M., 2010. Influence of carbon sources and C/N ratio on EPS production in anaerobic sequencing batch biofilm reactors for wastewater treatment. *Bioresour. Technol.* 101, 1324–1330.
- Murphy, J., Riley, J.P., 1962. A modified single solution method for the determination of phosphate in natural waters. *Anal. Chem. ACTA* 27, 31–36.
- Neu, L., Proctor, C.R., Walsler, J.-C., Hammes, F., 2019. Small-scale heterogeneity in drinking water biofilms. *Front. Microbiol.* 10, 2446.
- Neu, T.R., Manz, B., Volke, F., Dynes, J.J., Hitchcock, A.P., Lawrence, J.R., 2010. Advanced imaging techniques for assessment of structure, composition and function in biofilm systems. *FEMS Microbiol. Ecol.* 72, 1–21.
- Radu, A.I., Vrouwenvelder, J.S., van Loosdrecht, M.C.M., Picioreanu, C., 2012. Effect of flow velocity, substrate concentration and hydraulic cleaning on biofouling of reverse osmosis feed channels. *Chem. Eng. J.* 188, 30–39.
- Romano, S., Schulz-Vogt, H.N., González, J.M., Bondarev, V., 2015. Phosphate limitation induces drastic physiological changes, virulence-related gene expression, and secondary metabolite production in *Pseudovibrio* sp. strain FO-BEG1. *Appl. Environ. Microbiol.* 81, 3518–3528.
- Sanawar, H., Pinel, I., Farhat, N.M., Bucs, S.S., Zlopasa, J., Kruihof, J.C., Witkamp, G.J., van Loosdrecht, M.C.M., Vrouwenvelder, J.S., 2018. Enhanced biofilm solubilization by urea in reverse osmosis membrane systems. *Water Res. X* 1, 100004.
- Sevcenco, A.M., Paravidino, M., Vrouwenvelder, J.S., Wolterbeek, H.T., van Loosdrecht, M.C.M., Hagen, W.R., 2015. Phosphate and arsenate removal efficiency by thermostable ferritin enzyme from *Pyrococcus furiosus* using radioisotopes. *Water Res.* 76, 181–186.
- Seviour, T., Derlon, N., Dueholm, M.S., Flemming, H.-C., Girbal-Neuhausser, E., Horn, H., Kjelleberg, S., van Loosdrecht, M.C.M., Lotti, T., Malpei, M.F., Nerenberg, R., Neu, T.R., Paul, E., Yu, H., Lin, Y., 2019. Extracellular polymeric substances of biofilms: suffering from an identity crisis. *Water Res.* 151, 1–7.
- Shang, R., Verliefde, A.R.D., Hu, J., Heijman, S.G.J., Rietveld, L.C., 2014a. The impact of EOM, NOM and cations on phosphate rejection by tight ceramic ultrafiltration. *Separ. Purif. Technol.* 132, 289–294.
- Shang, R., Verliefde, A.R.D., Hu, J., Zeng, Z., Lu, J., Kemperman, A.J.B., Deng, H., Nijmeijer, K., Heijman, S.G.J., Rietveld, L.C., 2014b. Tight ceramic UF membrane as RO pre-treatment: the role of electrostatic interactions on phosphate rejection. *Water Res.* 48, 498–507.
- Siebrath, N., Farhat, N., Ding, W., Kruihof, J., Vrouwenvelder, J.S., 2019. Impact of membrane biofouling in the sequential development of performance indicators: feed channel pressure drop, permeability, and salt rejection. *J. Membr. Sci.* 585, 199–207.
- Sweity, A., Oren, Y., Ronen, Z., Herzberg, M., 2013. The influence of antiscalants on biofouling of RO membranes in seawater desalination. *Water Res.* 47, 3389–3398.
- Vrouwenvelder, J.S., Bakker, S.M., Wessels, L.P., van Paassen, J.A.M., 2007. The Membrane Fouling Simulator as a new tool for biofouling control of spiral-wound membranes. *Desalination* 204, 170–174.
- Vrouwenvelder, J.S., Beyer, F., Dahmani, K., Hasan, N., Galjaard, G., Kruihof, J.C., van Loosdrecht, M.C.M., 2010. Phosphate limitation to control biofouling. *Water Res.* 44, 3454–3466.
- Vrouwenvelder, J.S., Graf von der Schulenburg, D.A., Kruihof, J.C., Johns, M.L., van Loosdrecht, M.C.M., 2009. Biofouling of spiral-wound nanofiltration and reverse osmosis membranes: a feed spacer problem. *Water Res.* 43, 583–594.
- Vrouwenvelder, J.S., Manolarakis, S.A., van der Hoek, J.P., van Paassen, J.A.M., van der Meer, W.G.J., van Agtmaal, J.M.C., Prummel, H.D.M., Kruihof, J.C., van Loosdrecht, M.C.M., 2008. Quantitative biofouling diagnosis in full scale nanofiltration and reverse osmosis installations. *Water Res.* 42, 4856–4868.